

## Multiplicities in 100-GeV/c $\pi^+p$ and $pp$ Interactions Using a Tagged Beam\*

J. Erwin, J. H. Klems, W. Ko, R. L. Lander, D. E. Pellett, and P. M. Yager  
*Department of Physics, University of California, Davis, California 95616*

and

M. Alston-Garnjost  
*Lawrence Berkeley Laboratory, University of California, Berkeley, California 94720*  
 (Received 10 December 1973)

$\pi^+p$  and  $pp$  interactions at 100 GeV/c are studied in the National Accelerator Laboratory 30-in. bubble chamber with a tagged beam. Charged multiplicities in  $\pi^+p$  and  $pp$  interactions are compared. The average inelastic multiplicity of  $\pi^+p$  interactions is higher than for  $pp$  interactions ( $6.80 \pm 0.14$  versus  $6.49 \pm 0.10$ ). However, negative particle multiplicities for events with more than six charged particles follow Poisson statistics with similar means,  $2.56 \pm 0.09$  and  $2.61 \pm 0.08$ , for  $\pi^+p$  and  $pp$  interactions.

In this paper, we present results on charged-particle multiplicities from the analysis of approximately half of a 58 000-picture exposure of the National Accelerator Laboratory 30-in. hydrogen bubble chamber to a beam of  $(100.4 \pm 0.3)$ -GeV/c tagged positive particles. The secondary beam<sup>1</sup> was produced at  $0^\circ$  by an extracted 300-GeV proton beam and consisted of approximately 51%  $p$ , 44%  $\pi^+$ , 4%  $\mu^+$ , and 1%  $K^+$  (in the bubble chamber). This beam provided us a unique opportunity to compare  $\pi^+p$  and  $pp$  interactions under the same experimental conditions.

Although plastic scintillator hodoscopes have been devised<sup>2</sup> for tagging such beams, multiwire proportional chambers (MWPC) were used in this experiment. The beam particle tagging system consisted of a 35-m-long differential Cherenkov counter located 500 m upstream from the bubble chamber and three sets of MWPC located 175, 15, and 2.5 m upstream from the chamber. Each MWPC set consisted of three sensitive planes with 2-mm wire spacing. Wires on successive planes were rotated  $120^\circ$  about the beam axis with respect to the previous plane. The sensitive area of the set was a hexagon, 10 cm across. The Cherenkov counter determined the identity ( $p$ ,  $\pi$  or  $\mu$ , or  $K$ ) and the MWPC system the trajectory of each beam particle. This information was then correlated with the observed track positions in the bubble chamber photographs to identify the tracks.

We verified that the tagging system operated satisfactorily. There are two aspects to this verification: the Cherenkov counter and the correlation of tracks between the MWPC and the bubble chamber. Based on counting rates in the two photomultiplier tubes of the Cherenkov counter,

taken at various helium gas pressures, we estimate that 1% or less of the  $\pi^+$  signals were caused by  $\delta$  rays from beam protons. No correction has been made for this effect. The trajectory of a beam track can be reconstructed from the MWPC data 89% of the time. The 11% loss, due to upstream scattering, dead-time losses, spurious MWPC tracks, and MWPC failures, only causes loss of data, not biases. A sample of 1500 events was measured on the "spiral reader" at Lawrence Berkeley Laboratory and reconstructed using the program TVGP. Figure 1(a) shows the difference at the beginning of the chamber between the coordinate ( $y$ ) of the beam track in a plane perpendicular to the camera axis and the same quantity extrapolated from the tagging system. The full width at half-maximum is 1

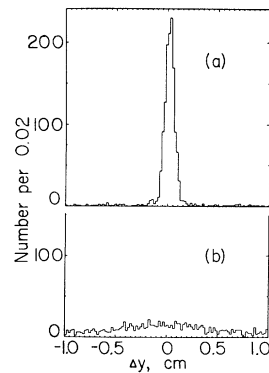


FIG. 1. Difference (in centimeters) between the coordinate of a beam track in the direction perpendicular to both the beam direction and the camera lens axis and the same quantity extrapolated from the MWPC. (a) The distance to the closest track, (b) the distance to the second-closest track. A total of 1500 beam tracks are involved.

mm. We find 84% of the beam tracks measured in the bubble chamber to have a MWPC reconstructed track lying within  $\pm 1$  mm in  $y$ . However, Fig. 1(b) shows that 12% of the bubble chamber tracks will have two MWPC tracks lying within  $\pm 1$  mm, of which half are resolved in the direction parallel to the camera axis. Only half of these ambiguous taggings are of different identities, leaving 3% ambiguous. Beam contamination due to the MWPC will occur when the real track fails to be tagged by the MWPC (16% of the time) and a track with a wrong identity satisfies the tagging criteria (3% of the time). Therefore, the misidentification of the beam due to the tagger alone would be about 0.5%. This 0.5% is eliminated by scanners noting two nearby tracks on the film when the tagger reports only one. Demanding that we tag a beam track unambiguously within  $\pm 1$  mm in  $y$ , we can use 81% of the beam tracks.

The film was scanned at a magnification of  $\frac{4}{3}$  life size. The fiducial volume was 47.4 cm along the beam and limited in the  $y$  direction by the 10-cm MWPC acceptance. The scanner counted the number of outgoing charged prongs (deleting obvious electrons and positrons) and recorded associated neutral decays. The scanner also determined the incident particle identity by measuring the distance between a fiducial mark and the beam track and comparing this to the MWPC prediction.

We observe a quite small number of odd-prong events (0.8%). They are events with proton recoils too short to see and/or one prong interacting very close to the primary vertex. We feel that secondary interactions almost never cause

TABLE I. Topological cross sections of inelastic scatterings.

Prong Numbers	$\pi^+p$ 100 GeV/c		pp 100 GeV/c		pp 102 GeV/c
	Numbers Observed	Cross Sections (mb)	Numbers Observed	Cross Sections (mb)	Cross Sections (mb)
2		$2.8 \pm 0.7$		$4.6 \pm 0.7$	$4.8 \pm 0.6$
4	285	$4.12 \pm 0.25$	604	$7.54 \pm 0.31$	$8.1 \pm 0.5$
6	384	$5.54 \pm 0.29$	624	$7.73 \pm 0.31$	$7.6 \pm 0.5$
8	306	$4.42 \pm 0.25$	541	$5.58 \pm 0.26$	$5.8 \pm 0.4$
10	192	$2.77 \pm 0.20$	315	$3.90 \pm 0.22$	$3.5 \pm 0.3$
12	104	$1.50 \pm 0.15$	162	$2.01 \pm 0.16$	$2.0 \pm 0.3$
14	38	$0.55 \pm 0.09$	63	$0.78 \pm 0.10$	$0.70 \pm 0.15$
16	16	$0.23 \pm 0.06$	25	$0.31 \pm 0.06$	$0.19 \pm 0.08$
18	6	$0.09 \pm 0.04$	5	$0.06 \pm 0.04$	$0.10 \pm 0.05$
20	2	$0.03 \pm 0.02$	3	$0.04 \pm 0.03$	--
All		$22.0 \pm 0.9$		$32.5 \pm 0.9$	$32.8 \pm 1.1$

miscounting when they occur in low-multiplicity events. Therefore, low-multiplicity odd prongs are increased in prong number by one because of invisible proton recoils. The higher-prong events are more susceptible to error from secondary interactions, and their prong numbers should be decreased. We have arbitrarily chosen seven prongs as the dividing point. All odd-prong events with prong number seven and larger have been assigned a prong count three less than that observed.<sup>3</sup> The scanning efficiency for four-prong and higher multiplicities was 99%, and for two prongs was 93%.<sup>4</sup> These corrections have been made.

The inelastic two-prong cross sections were estimated by using the optical point and fitting the observed recoil-proton  $t$  distributions of a sample of measured events to a function with two terms, one for the elastic and another for the inelastic events. Details will be presented in a later paper.

The topological cross sections for 100-GeV/c  $\pi^+p$  and  $pp$  interactions from this experiment are shown in Table I. These are based on a liquid-hydrogen density of  $0.0630 \pm 0.0006$  gm/cm<sup>3</sup> as measured in these photos, and are corrected for muon contamination [(7.6  $\pm$  1.7)%]<sup>5</sup> in the  $\pi^+p$  events. Also shown are existing  $pp$  data at 102 GeV/c.<sup>6</sup> The data from the two experiments agree within the accuracy of the measurements.

In Fig. 2 we show the variations of multiplicity of  $\pi^+p$  interactions as functions of momentum.<sup>7-10</sup> We see that four-prong cross sections continue to decrease, the six-prong have peaked out, and

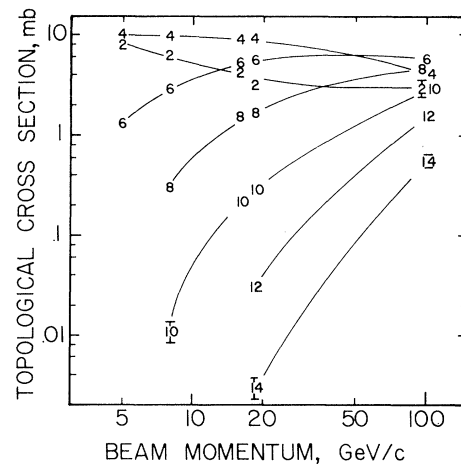


FIG. 2. Topological cross sections of  $\pi^+p$  interactions as a function of incident momentum. Where error bars are not shown, they are smaller than the symbols. The lines are merely to guide the eye.

all the higher-prong are rising at 100 GeV/c. It is interesting that the two-prong cross section seems to have almost stopped decreasing. This may imply a dominance of diffraction in the two-prong events.

The average multiplicity in the inelastic  $\pi^+p$  interaction is  $6.80 \pm 0.14$ , significantly higher than  $6.49 \pm 0.10$  in the  $pp$  interaction. This difference is also observed in the comparison of  $\pi^-p$ <sup>11</sup> and  $pp$ <sup>12</sup> interactions at 200 GeV/c, where average multiplicities are  $8.02 \pm 0.12$  and  $7.65 \pm 0.17$ , respectively.

The squares of the standard deviation for the distributions of the  $\pi^-$  produced in the  $\pi^+p$  and  $pp$  interactions from the table are  $2.72 \pm 0.10$  and  $2.69 \pm 0.07$ , higher than the mean numbers of  $\pi^-$ 's ( $2.40 \pm 0.07$  and  $2.25 \pm 0.05$ ). Thus the distributions are wider than the Poisson form which is predicted by many short-range-correlation models.<sup>13</sup> However, the discrepancies occur only at low multiplicities, as can be illustrated in the following way.<sup>14</sup> With a Poisson distribution,

$$\sigma_n = \sigma_{\text{inel}} \langle n \rangle^n e^{-\langle n \rangle} / n!,$$

where  $n$  is the number of  $\pi^-$ 's,  $\ln(n! \sigma_n)$  will be linear in  $n$  with a slope of  $\ln \langle n \rangle$ . Figure 3 is such a plot and shows that  $\ln(n! \sigma_n)$  is indeed linear for  $n$  larger than 2, with an excess at small  $n$ . The confidence levels for straight-line fits to  $n$  greater than 2 are 96% for  $\pi^+p$  and 81% for  $pp$ . A significant excess is observed in the low multiplicities for  $pp$  interactions. This observation agrees well with the two-component models,<sup>14,15</sup> with the

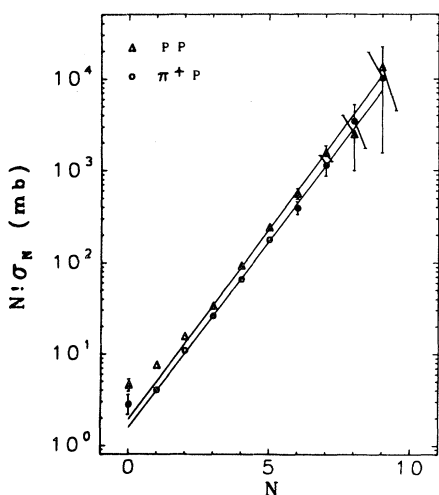


FIG. 3. The quantity  $n! \sigma_n$  versus  $n$ .  $n$  is the number of  $\pi^-$  secondaries. The straight lines are the fits to points with  $n > 2$ .

higher component obeying a Poisson distribution and a second component dominating at lower multiplicities. The excess in the  $\pi^+p$  interactions is observed only in the case where no  $\pi^-$  is produced; so if two components exist, their distributions must be similar or the second one is small.

It is worth noting that the two straight lines in Fig. 3 are nearly parallel. The higher components ( $n$  greater than 3) of  $\pi^+p$  and  $pp$  interactions have similar  $\pi^-$  multiplicities of  $2.56 \pm 0.09$  and  $2.61 \pm 0.08$ , respectively. We used this technique to compare  $\pi^-p$  and  $pp$  interactions at 200 GeV/c,<sup>11,12</sup> and also obtained similar  $\pi^-$  multiplicities of  $3.38 \pm 0.10$  and  $3.43 \pm 0.10$ , respectively, for the higher components.

We remind the reader that the analysis reported here is based on the efforts of a large number of individuals at the National Accelerator Laboratory, at the universities of the Proportional Hodoscope System Consortium, at the University of California at Davis, at the Lawrence Berkeley Laboratory, and within the U. S. Atomic Energy Commission agencies. The authors are pleased to acknowledge this joint effort.

\*Work supported in part by the U. S. Atomic Energy Commission.

<sup>1</sup>J. Lach and S. Pruss, NAL Internal Report No. TM-285, 1971 (unpublished).

<sup>2</sup>See, for example, D. Pellett, J. Erwin, D. Faulkner, W. Ko, R. L. Lander, and P. M. Yager, to be published.

<sup>3</sup>Secondary interactions here are observed to have an average multiplicity of  $\sim 4$ .

<sup>4</sup>We required that the proton recoil be at least 0.2 in. long on the scan table in at least one view.

<sup>5</sup>J. Klems, University of California at Davis Report No. UCD-PPL-11/7/73 (unpublished).

<sup>6</sup>J. W. Chapman, N. Green, B. P. Roe, A. A. Seidel, D. Sinclair, J. C. Vander Velde, C. M. Bromberg, D. Cohen, T. Ferbel, P. Slattery, S. Stone, and B. Werner, Phys. Rev. Lett. **29**, 1686 (1972).

<sup>7</sup>L. Bondar, K. H. Eichel, H. Kaufmann, K. Lannis, R. Leiste, R. Pose, K. Bockmann, U. Gouth, K. Steinberger, B. Nellen, V. Blobel, H. Butenschon, I. Damann, P. Handel, E. Lohrmann, P. Schilling, G. Wolf, N. N. Biswas, N. Chmitz, and I. Weigl, Nuovo Cimento **44A**, 530 (1966).

<sup>8</sup>M. Aderholz, M. Deutschmann, E. Keppel, G. Kraus, H. Weber, C. Grote, H. H. Kaufmann, S. Novak, M. Walter, H. Bottcher, T. Byer, V. T. Cocconi, P. F. Dalpiaz, J. D. Hansen, G. Kellner, W. Kittel, M. Markyton, A. Bihul, D. R. O. Morrison, and H. Tofte, Nucl. Phys. **B8**, 45 (1968).

<sup>9</sup>Aachen-Berlin-Bonn-CERN-Cracow-Warsaw Collaboration (1971).

<sup>10</sup>J. T. Powers, N. N. Biswas, N. M. Cason, V. P.

Kennery, and W. D. Shephard, Phys. Rev. D 3, 1947 (1973).

<sup>11</sup>D. Bogart, R. Hanft, F. R. Huson, D. Ljung, C. Pascaud, S. Pruss, W. M. Smart, G. S. Abrams, H. H. Bingham, D. M. Chew, B. Y. Daugéras, W. B. Fretter, C. E. Friedberg, G. Goldhaber, W. R. Graves, A. D. Johnson, J. A. Kadyk, L. Stutte, G. H. Trilling, F. C. Winkelmann, and G. P. Yost, Phys. Rev. Lett. 31, 1271 (1973).

<sup>12</sup>G. Charlton, Y. Cho, M. Derrick, R. Engelmann, T. Fields, L. Hyman, K. Jaeger, U. Mehtani, B. Mus-

grave, Y. Oren, D. Rhines, P. Schreiner, H. Yuta, L. Voyvodic, R. Walker, J. Whitmore, H. B. Crawley, Z. M. Ma, and R. G. Glasser, Phys. Rev. Lett. 29, 515 (1972).

<sup>13</sup>For example, C. P. Wang, Phys. Rev. 180, 1463 (1969); C. DeTar, Phys. Rev. D 3, 128 (1971).

<sup>14</sup>W. R. Frazer, R. D. Peccei, S. S. Pinsky, and C.-I. Tan, Phys. Rev. D 7, 2647 (1973).

<sup>15</sup>K. G. Wilson, Cornell University Report No. CLNS-131, 1970 (unpublished); J. Lach and E. Malamud, Phys. Lett. 44B, 474 (1973).

## Diffractive Component in $pp$ Collisions at 102 and 405 GeV\*

J. W. Chapman, J. W. Cooper, N. Green, A. A. Seidl, and J. C. Vender Velde  
*University of Michigan, Ann Arbor, Michigan 48104*

and

C. M. Bromberg, D. Cohen,† T. Ferbel,‡ and P. Slattery  
*University of Rochester, Rochester, New York 14627*  
(Received 29 November 1973)

We study the diffractive component in  $pp$  collisions at 102 and 405 GeV and examine its energy dependence in  $M^2$  and  $x$  variables. The total cross section for  $|x| > 0.9$  remains approximately constant:  $6.6 \pm 0.5$  and  $6.8 \pm 0.7$  mb at the two energies. However, both  $d\sigma/dx$  and  $d\sigma/dM^2$  show strong energy dependence within the  $|x| > 0.9$  region. The energy and  $M^2$  dependences of  $d\sigma/dM^2$  do not have the characteristics of a triple-Pomeron term for  $0.90 < |x| < 0.99$ .

Recent studies of the recoil-proton spectrum observed in  $pp$  collisions at high energies have provided evidence for the presence of a sizable inelastic diffractive component in the data.<sup>1</sup> Furthermore, the universal aspect of diffractive production in hadronic collisions has been revealed through investigations utilizing  $\pi p$  incident channels.<sup>2</sup> In this paper we discuss our complete results at 102 GeV pertaining to diffractive production in the reaction

$$p + p \rightarrow p + \text{anything.} \quad (1)$$

We also present our preliminary findings for this inclusive process at 405 GeV.

Our data are from the 30-in. hydrogen bubble chamber at the National Accelerator Laboratory (NAL): a 30 000-picture exposure at 102 GeV/c and an initial 12 000-picture exposure at 405 GeV/c, yielding 124 and 65 events/mb, respectively. The film was scanned three times for events having a possible proton with bubble density greater than 1.5 times the minimum. All such candidate tracks were measured, reconstructed, and subsequently reexamined to identify protons

through their predicted ionization. This identification is reliable up to a lab momentum of about 1.3 GeV/c, consequently a final cut at 1.2 GeV/c was imposed on the data. Because of the sharp transverse-momentum ( $P_T$ ) dependence of Reaction (1), this cut does not cause any significant bias in the data we present for values of  $x < -0.5$ . ( $x$  is defined as  $P_{\parallel}/P_{\text{incident}}$  in the c.m. system.)

Two-prong inelastic events were separated from elastic events by a kinematic fitting procedure.<sup>3</sup> Elastic background was further reduced by requiring the square of the missing mass ( $M$ ) recoiling from the proton in Reaction (1) to be greater than 1 and  $-1$  GeV<sup>2</sup> at 102 and 405 GeV, respectively. (The average resolution in  $M^2$  is  $\pm 0.7$  and  $\pm 2.8$  GeV<sup>2</sup>, corresponding to  $\delta x = \pm 0.0035$  at the two beam energies.) Small corrections were applied to the two-prong events to account for the resulting losses. Scanning-loss corrections, based on the loss found for elastic events, were also applied to the two-prong data for short protons with  $|t| < 0.04$  GeV<sup>2</sup>. Small corrections were also applied for a few  $\geq 4$ -prong events which had protons too short to see and/or mea-